OPEN ACCESS
JOURNAL OF ADVANCED DIELECTRICS
Vol. 11, No. 6 (2021) 2150029 (6 pages)
© The Author(s)
DOI: 10.1142/S2010135X21500296

Photocatalytic degradations of JWS-type kinetics

C. L. Wang
School of Physics, Shandong University, Jinan
Shandong 250100, P. R. China
wangcl@sdu.edu.cn

Received 30 September 2021; Revised 19 October 2021; Accepted 29 October 2021; Published 2 December 2021

Photocatalytic degradation kinetics of Jurlewicz–Weron–Stanislavsky (JWS) type has been identified. Experimental data are taken from previous published works, and fitted with the JWS relaxation function as well as that of the Havriliak–Negami (HN) model. All experimental data can fit with either model fairly good. From the fitting parameters, the Jonscher indices are calculated and Jonscher diagram is plotted for the chemical kinetics of photocatalytic degradations. This work suggests that material parameters of photocatalysts can be well defined in the sense of fractional calculus.

Keywords: Photocatalytic degradation; JWS relaxation; Jonscher index; fractional calculus.

1. Introduction

Chemical reaction kinetics of the catalytic degradation process with Cole–Cole, Cole–Davidson and Havriliak–Negami (HN) models have been identified in previous works.[1–3] Though these kinetic models have been proposed for understanding the dielectric relaxation process,[4] they can be applied to chemical reaction kinetics quite successfully. Within the framework of universal relaxation law, a novel type of model, i.e., the Jurlewicz–Weron–Stanislavsky (JWS) relaxation, has been proposed.[5–8] This model has been applied to dielectric dispersion of $NH_4H_2PO_4$ crystals quite successfully.[5] The corresponding time-domain functions, i.e., response function and relaxation function, of all these models have also been worked out recently in the sense of fractional calculus.[9] To identify the experimental evidence of the JWS model in chemical reaction kinetics, experimental data of photocatalytic degradations in published works are selected to fit the time-domain functions. Then the Jonscher indices are obtained from the fitting parameters, and Jonscher diagram is plotted for these photocatalysts.

2. Fittings and Results

Basically there are two types of kinetic models, i.e., HN and JWS models. The other models can be regarded as specific cases of these two models. Therefore, the relaxation functions of these two models are used in this work. The time t dependence of pollutant concentration $C(t)$ in catalytic degradation process can be written as

$$\frac{C_{\mathrm{HN}}(t)}{C_0} = 1 - \left(\frac{t}{\tau}\right)^{\alpha\gamma} E^{\gamma}_{\alpha,\alpha\gamma}\left(-\left(\frac{t}{\tau}\right)^{\alpha}\right) \tag{1}$$

$$\frac{C_{\mathrm{JWS}}(t)}{C_0} = E^{\gamma}_{\alpha,1}\left(-\left(\frac{t}{\tau}\right)^{\alpha}\right), \tag{2}$$

where the subscript HN stands for the HN model and subscript JWS denotes the JWS model, C_0 is the initial value of pollutant concentration and τ is the characteristic degradation time. Model parameters α and γ are related with the order of the derivative. Function $E^{\gamma}_{\alpha,\beta}(\cdot)$ is the three-parameter Mittag-Leffler function, or Prabhakar function.[10–12] For any $z \in C$, this function is defined as

$$E^{\gamma}_{\alpha,\beta}(z) = \frac{1}{\Gamma(\gamma)} \sum_{k=0}^{\infty} \frac{\Gamma(\gamma+k)}{k!\,\Gamma(\alpha k+\beta)} z^k \tag{3}$$

$$\alpha, \beta, \gamma \in \mathrm{C}, \quad \mathrm{Re}(\alpha) > 0.$$

where $\Gamma(\cdot)$ denotes the Euler's gamma function.

The fitting approach with experimental data is similar to previous works.[1–3] Both HN model of Eq. (1) and JWS model of Eq. (2) are fitted with the experimental data. Only the results with reasonable values of model parameters are kept and presented here. The first experimental dataset is of the photocatalytic degradations of ciprofloxacin (CIP) by graphitic carbon nitride (g-C_3N_4) and copper-doped carbon nitride (Cu–g-C_3N_4).[13] Second experimental dataset is of an organic photocatalyst, i.e., *N*,*N*′-bis(propionic acid)-perylene-3,4,9,10-tetracarboxylic diimide hybridized sulfur-doped carbon nitride (PDI-Ala–S–C_3N_4) with S-scheme heterojunction, for the degradation of tetracycline (TC).[14] Third dataset is about the reproducibility of Rhodamine B (RhB) degradation under solar light using

This is an Open Access article published by World Scientific Publishing Company. It is distributed under the terms of the Creative Commons Attribution 4.0 (CC BY) License which permits use, distribution and reproduction in any medium, provided the original work is properly cited.

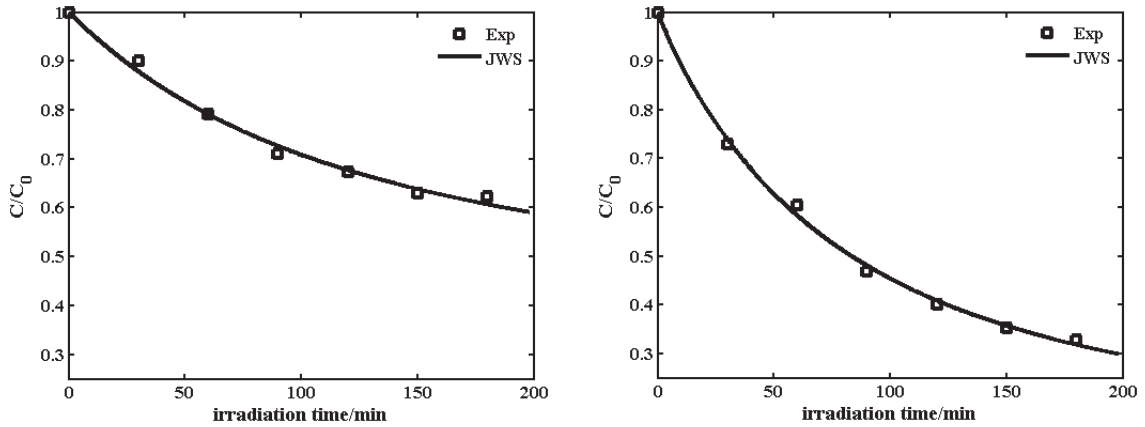

Fig. 1. Solid lines for JWS model and square symbols for experimental data[13]: (a) CIP degradation by g-C_3N_4 and (b) CIP degradation by Cu–g-C_3N_4.

Table 1. Fitting parameters and Jonscher indices.

Catalyst	τ (min)	α	γ	m	n	Model	Source
g-C_3N_4	53.76	1	0.26	0.26	0	JWS	Ref. 13
Cu–g-C_3N_4	55.79	0.94	0.57	0.54	0.06	JWS	Ref. 13
20% PDI-Ala–S–C_3N_4	42.65	1	0.95	0.95	0	JWS	Ref. 14
30% PDI-Ala–S–C_3N_4	36.63	1	0.94	0.94	0	JWS	Ref. 14
40% PDI-Ala–S–C_3N_4	47.60	1	0.88	0.88	0	JWS	Ref. 14
50% PDI-Ala–S–C_3N_4	53.62	1	0.78	0.78	0	JWS	Ref. 14
Nb–$BiVO_4$: Pristine	489.11	1	0.66	1	0.34	HN	Ref. 15
Nb–$BiVO_4$: First run	22.95	1	0.42	0.42	0	JWS	Ref. 15
Nb–$BiVO_4$: Second run	363.70	1	0.65	1	0.35	HN	Ref. 15
Nb–$BiVO_4$: Third run	1063.9	1	0.60	1	0.40	HN	Ref. 15
Co–$CuBi_2O_4$: pH=4.5	6.92	0.96	0.49	0.96	0.53	HN	Ref. 16
Co–$CuBi_2O_4$: pH=7	1.01	1	0.89	0.89	1	JWS	Ref. 16
Co–$CuBi_2O_4$: pH=9.5	1.14	0.99	0.65	0.99	0.34	HN	Ref. 16
Co–$CuBi_2O_4$: Cycle 1	1.46	1	0.99	0.99	0.03	JWS	Ref. 16
Co–$CuBi_2O_4$: Cycle 2	1.41	1	0.91	0.91	0.03	JWS	Ref. 16
Co–$CuBi_2O_4$: Cycle 3	1.56	0.97	0.91	0.88	0.03	JWS	Ref. 16

niobium-doped bismuth vanadate.[15] Last experimental dataset is about the effects of pH values on the degradation of sulfanilamide (SA), and the reusability of Co–$CuBi_2O_4$ for SA removal via peroxymonosulfate (PMS) activation over different cycles.[16]

Fitting curves for the degradations of CIP by g-C_3N_4 and Cu–g-C_3N_4 are shown in Fig. 1, and the fitting parameters are listed in Table 1. It can be easily found that JWS model fits the degradations very well. Both degradation curves deviate seriously from the standard integer first-order chemical reaction kinetics, i.e., $g = 0.26$ and 0.57, respectively.

Also listed in Table 1 are the Jonscher indices m and n, which can be calculated from the parameters α and γ.[17] Jonscher indices are introduced by Jonscher in describing the universal dielectric relaxation law.[18,19] A diagram is plotted using the two Jonscher indices, i.e., referred to as the Jonscher diagram.[17–20] Each kinetics or relaxation process corresponds to a point in the Jonscher diagram. The point at the top-right corner stands for the integer first-order chemical reaction kinetics, as shown in Fig. 2. The upper triangular region stands for the HN kinetics, and the lower triangular region represents the JWS kinetics. The degradations of CIP by g-C_3N_4 and Cu–g-C_3N_4 are denoted with symbols of open circles in Fig. 2. It is quite obvious that they are of JWS-type kinetics and deviate seriously from the standard integer first-order kinetics process.

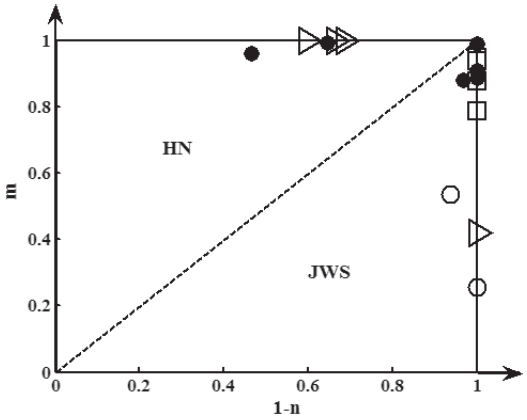

Fig. 2. Jonscher diagram for the chemical reaction kinetics of photocatalytic degradations. HN stands for Havriliak–Negami model, and JWS for the Jurlewicz–Weron–Stanislavsky model. Symbols are for different photocatalysts.

Fitting curves for the degradation of TC by PDI-Ala–S–C_3N_4 heterojunctions are shown in Fig. 3 for different contents of PDI-Ala. All the degradations are of JWS type. An interesting issue is that all these degradation processes are on the right edge of the Jonscher diagram, shown as symbols of open squares in Fig. 2. These degradations do not deviate from the standard integer first-order kinetics very much, as they are very close to the point at the top-right corner. Especially for the catalysts of 20% PDI-Ala–S–C_3N_4 and 30% PDI-Ala–S–C_3N_4, the values of Jonscher index m are 0.95 and 0.94, respectively, that are very close to 1.

Bismuth vanadate has been gaining stronger interest in the photochemical community, since it is a solar-driven photocatalyst.[14] Reproducibility of photocatalytic measurements and the reusability of photocatalysts are crucial parameters in the efficiency of photodegradation processes. The reproducibility of Nb-doped $BiVO_4$ on the degradation of RhB is shown in Fig. 4 for different runs. Fitting parameters are listed in Table 1. It has to be pointed that degradation by pristine $BiVO_4$ is of the HN-type kinetics. But the first run of degradation by Nb–$BiVO_4$ changes to the JWS-type kinetics. After repeated use, the photocatalytic degradation changes back to HN type again. The degradation types are shown as right-triangles on the Jonscher diagram of Fig. 2. Jonscher index of first run is on the right edge, and Jonscher indices of pristine and second and third runs are on the top edge. The most efficient degradation happens in the first run, as can be

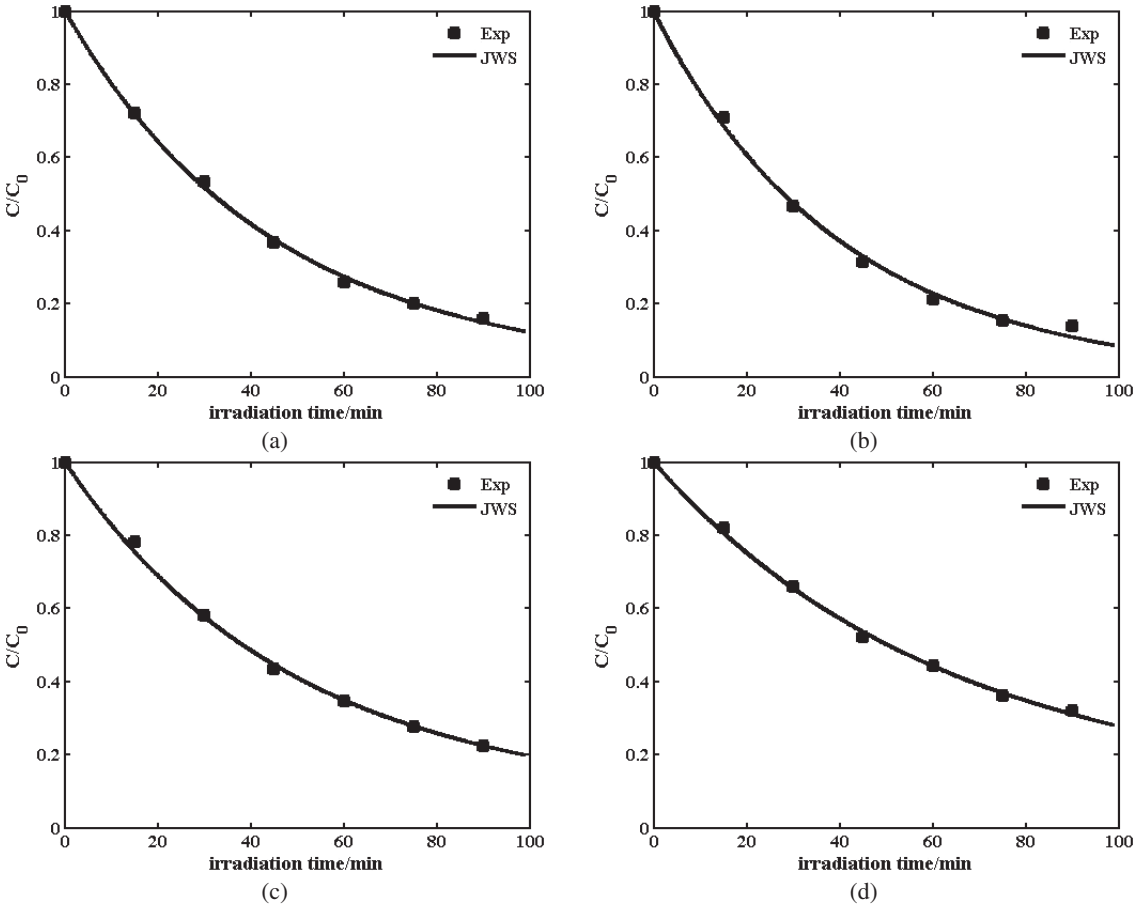

Fig. 3. Solid lines for the JWS model and square symbols for experimental data[14]: (a) 20% PDI-Ala–S–C_3N_4, (b) 30% PDI-Ala–S–C_3N_4, (c) 40% PDI-Ala–S–C_3N_4 and (d) 50% PDI-Ala–S–C_3N_4.

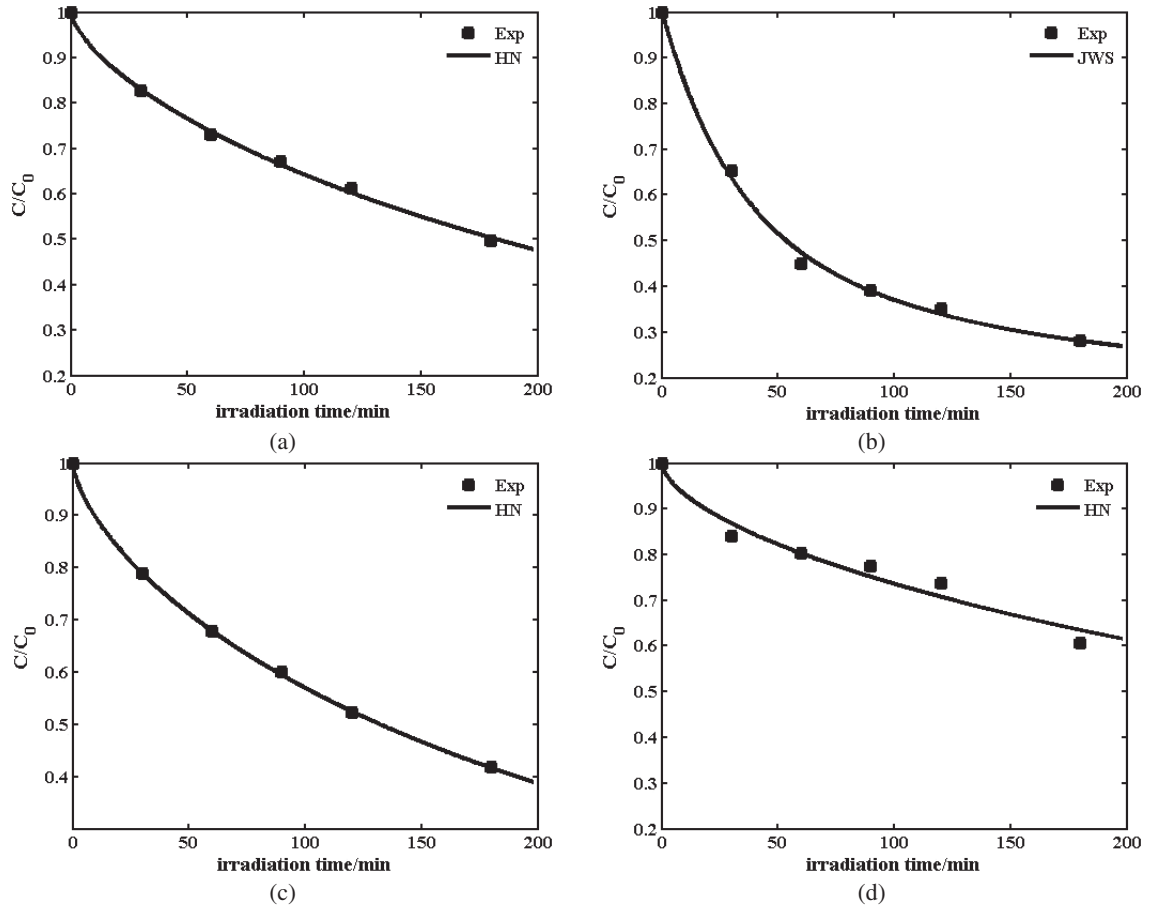

Fig. 4. Reproducibility of Nb–$BiVO_4$ on the degradation of RhB. Solid lines for fitting with either JWS or HN model and square symbols for experimental data[15]: (a) pristine, (b) first run, (c) second run and (d) third run.

seen in Fig. 4(b). This also can be easily confirmed by the degradation time τ in Table 1, since it is the shortest one.

Degradations of SA by Co–$CuBi_2O_4$ at different pH values are shown in Figs. 5(a)–5(c), and the reusability of Co–$CuBi_2O_4$ for SA removal at different cycles is shown in Figs. 5(d)–5(f). The interesting point is that for either acidic or alkaline solution, the degradation is of HN type, as shown in Figs. 5(a) and 5(c). But the degradation is of JWS type in pH-neutral solution, as shown in Fig. 5(b). The degradation is always of JWS type at different reuse cycles, as shown

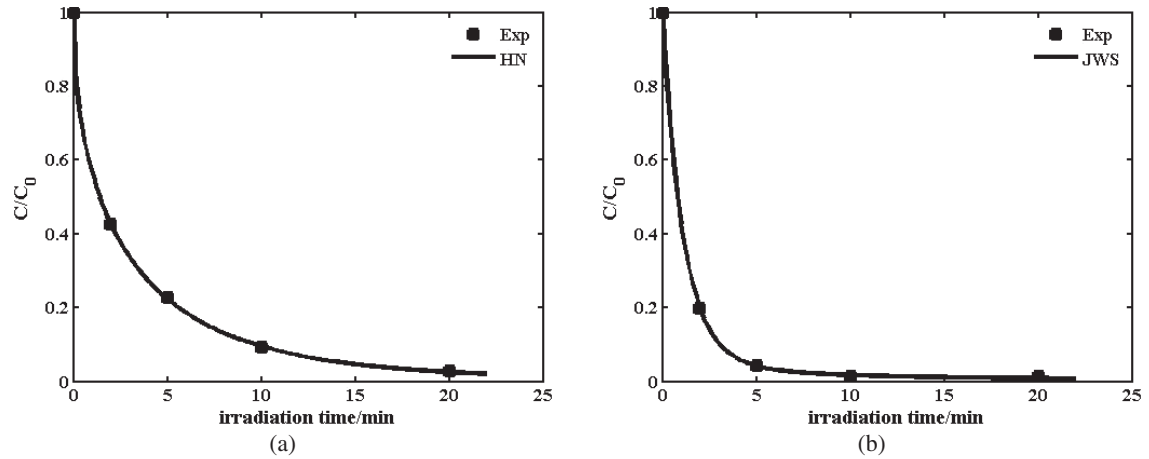

Fig. 5. Effects of pH value on the degradation of SA: (a) pH=4.5, (b) pH=7 and (c) pH=9.5. Reusability for SA removal: (d) cycle 1, (e) cycle 2 and (f) cycle 3. Solid lines are for fitting with either JWS or HN model and square symbols are for experimental data.[16]

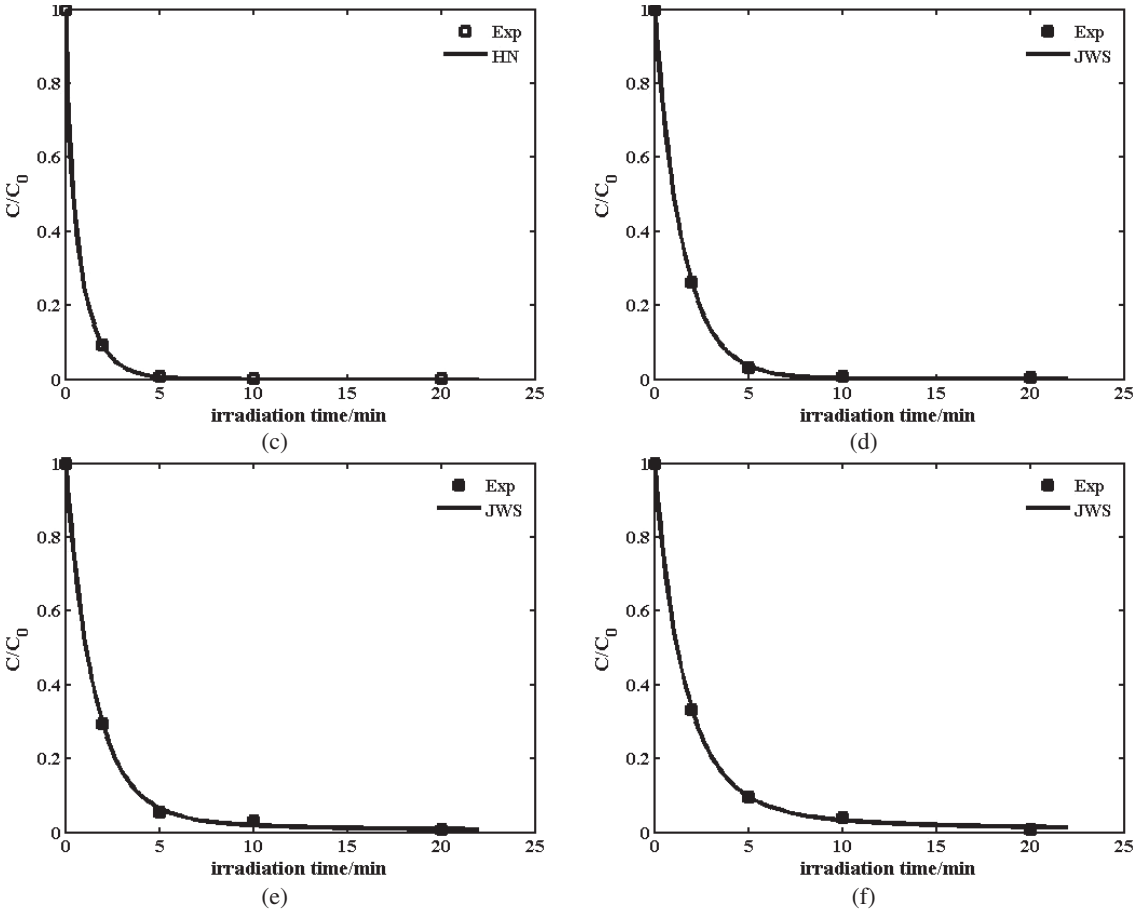

Fig. 5. (*Continued*)

in Figs. 5(d)–5(f). All the JWS-type degradations by Co–$CuBi_2O_4$ are quite close as the integer first-order chemical reaction kinetics, denoted as solid circles in Fig. 2. This also can be easily seen from the last six rows in Table 1, where both α and γ are equal or quite close to 1 for the degradations in these cycles.

Together with previous works,[1–3] all the kinetic types are identified in the photocatalytic degradation processes. That means that photocatalytic degradation process can be well analyzed by fractional calculus. Different degradation types of a photocatalytic process can be easily determined from the Jonscher index and Jonscher diagram.

3. Summary

Chemical reaction kinetics of the Jurlewicz–Weron–Stanislavsky type has been identified in photocatalytic degradations. The obtained Jonscher indices are shown in the Jonscher diagram, which includes all the fractional kinetic types. Photocatalytic degradations can be well described by fractional first-order kinetics. Degradation characteristic time as well as Jonscher index can serve as well-defined material constants for the degradation of photocatalysts.

Acknowledgments

This work is supported by the National Natural Science Foundation of China (51672159, 51501105 and 51611540342).

References

[1]C. L. Wang, Fractional kinetics of photocatalytic degradation, *J. Adv. Dielectr*. **08**, 1850034 (2018).
[2]C. L. Wang, Photocatalytic degradation as Davidson–Cole relaxation in time domain, *J. Adv. Dielectr.* **09**, 1950006 (2019).
[3]C. L. Wang, Piezo-catalytic degradation of Havriliak–Negami type, *J. Adv. Dielectr.* **09**, 1950021 (2019).
[4]V. Uchaikin and R. Sibatov, *Fractional Kinetics in Solids* (World Scientific, Singapore, 2013).
[5]A. Stanislavsky, K. Weron and J. Trzmiel, Subordination model of anomalous diffusion leading to the two-power-law relaxation responses, *Europhys. Lett.* **91**, 40003 (2010)
[6]A. Jurlewicz, J. Trzmiel and K. Weron, Two-power-law relaxation processes in complex materials, *Acta Phys. Pol. B* **41**, 1001 (2010).
[7]J. Trzmiel, A. Jurlewicz and K. Weron, The frequency-domain relaxation response of gallium doped $Cd_{1-x}Mn_xTe$, *J. Phys., Condens. Matter* **22**, 095802 (2010).
[8]J. Trzmiel, T. Marciniszyn and J. Komar, Generalized Mittag-Leffler relaxation of $NH_4H_2PO_4$: Porous glass composite, *J. Non-Cryst. Solids* **357**, 1791 (2011).

[9]R. Garrappa, F. Mainardi and G. Maione, Models of dielectric relaxation based on completely monotone functions, *Fract. Calc. Appl. Anal.* **19**, 1105 (2016).
[10]R. Gorenflo, A. A. Kilbas, F. Mainardi and S. V. Rogosin, *Mittag-Leffler Functions, Related Topics and Applications*, 2nd edn. (Springer-Verlag, Berlin, 2020).
[11]R. Garra and R. Garrappa, The Prabhakar or three parameter Mittag-Leffler function: Theory and application, *Commun. Nonlinear Sci. Numer. Simul.* **56**, 314 (2018).
[12]A. Giusti, I. Colombaro, R. Garra, R. Garrappa, F. Polito, M. Popolizio and F. Mainardi, A practical guide to Prabhakar fractional calculus, *Fract. Calc. Appl. Anal.* **23**, 9 (2020).
[13]X. W. Li, B. Wang, W. X. Yin, J. Di, J. X. Xia, W. S. Zhu and H. M. Li, Cu^{2+} modified g-C_3N_4 photocatalysts for visible light photocatalytic properties, *Acta Phys.-Chim. Sin.* **36**, 1902001 (2020).
[14]X. B. Li, J. Y. Liu, J. T. Huang, C. Z. He, Z. J. Feng, Z. Chen, L. Y. Wan and F. Deng, All organic S-scheme heterojunction PDI-Ala–S–C_3N_4 photo-catalyst with enhanced photocatalytic performance, *Acta Phys.-Chim. Sin.* **37**, 2010030 (2021).
[15]O. Monfort and G. Plesch, Bismuth vanadate-based semiconductor photo-catalysts: A short critical review on the efficiency and the mechanism of photo-degradation of organic pollutants, *Environ. Sci. Pollut. Res.* **25**, 19362 (2018).
[16]W. D. Oh, Z. L. Dong and T. T. Lim, Hierarchically-structured Co-$CuBi_2O_4$ and Cu-$CuBi_2O_4$ for sulfanilamide removal via peroxymonosulfate activation, *Catal. Today* **280**, 2 (2017).
[17]C. L. Wang, Jonscher indices for dielectric materials, *J. Adv. Dielectr.* **09**, 1950046 (2019).
[18]A. K. Jonscher, *Dielectric Relaxation in Solids* (Chelsea Dielectrics Press, 1983); A. K. 琼克, 固体中的介电弛豫 (西安交通大学出版社, 西安, 2008).
[19]A. K. Jonscher, *Universal Relaxation Law* (Chelsea Dielectrics Press, 1996); A. K. 琼克, 普适弛豫定律体 (西安交通大学出版社, 西安, 2008).
[20]A. Stanislavsky and K. Weron, Stochastic tools hidden behind the empirical dielectric relaxation laws, *Rep. Prog. Phys.* **80**, 036001 (2017).